Carbohydrate Polymers 88 (2012) 596–603

Contents lists available at SciVerse ScienceDirect

Carbohydrate Polymers

journal homepage: www.elsevier.com/locate/carbpol

Water holding and release properties of bacterial cellulose obtained by in situ and ex situ modification

Mazhar Ul-Islam[a], Taous Khan[a,b], Joong Kon Park[a,*]

[a] Department of Chemical Engineering, Kyungpook National University, Daegu 702-701, South Korea
[b] Department of Pharmacy, COMSATS Institute of Information Technology, Abbottabad, Pakistan

ARTICLE INFO

Article history:
Received 25 November 2011
Received in revised form
27 December 2011
Accepted 1 January 2012
Available online 11 January 2012

Keywords:
Bacterial cellulose
Water holding capacity
Water release rate
Pore size
In situ and ex situ modifications

ABSTRACT

The biomedical applications of bacterial cellulose (BC) as a dressing material are mainly dependent on its water holding capacity (WHC) and water release rate (WRR), which in turn depend on pore size, pore volume and surface area. In the present study, the effects of structural modifications (in situ and ex situ) of BC on the WHC and WRR were investigated. The in situ modified BC was produced by the addition of various concentrations of a single sugar α-linked glucuronic acid-based oligosaccharide (SSGO) to the culture media while the ex situ modifications were carried out by preparing BC composites with chitosan (Ch) and montmorillonite (MMT). The morphological characteristics of the modified BC samples were studied with FE-SEM while their pore size, pore volume and surface area were determined through BET analysis. The results showed modifications in micro-fibril arrangements, pore size, pore volume and surface area in all BC samples compared to the control. The in situ modified BC showed denser fibril arrangement and decreasing pore size and pore volume with increasing SSGO concentration. Pore size and volume were also reduced in BC composites, probably due to the filling of pores by MMT and Ch. The variations in the WHC and WRR of BC samples were correlated to changes in various parameters after structural modifications. The WHC and WRR increased with pore volume and pore size in in situ modified BC samples. In ex situ modified BC, the WHC and WRR were dependent on the nature and arrangement of the composite materials on the surface and in the matrix of the BC sheets.

1. Introduction

Bacterial cellulose (BC) is a fascinating biomaterial with distinctive properties, including high water holding capacity, crystallinity, tensile strength, an ultrafine fibre network and the ability to be molded into three-dimensional (3D) structures during synthesis (Choi, Song, Kim, Chang, & Ki, 2009; Li, Kim, Lee, Kee, & Oh, 2011; Nasab & Yousef, 2010). The most exciting applications of BC are in biomedical fields, such as wound dressing materials (Cienchanska, 2004; Czaja, Krystynowicz, Bielecki, & Brown, 2006), artificial skin, vascular grafts, scaffolds for tissue engineering, artificial blood vessels, medical pads and dental implants (Czaja, Young, Kawechi, & Brown, 2007; Klemn, Schumann, Udhardt, & Marsch, 2001; Shezad, Khan, Khan, & Park, 2009; Wan, Hutter, Millon, & Guhados, 2006), although it is also widely used in the food, paper, acoustic, filter membrane, and pharmaceutical industries (Phisalaphong, Suwanmajo, & Sangtherapitiku, 2008).

BC fibrils are about 100 times smaller than plant cellulose. The well separated nano-fibrils of BC create an expanded surface area and highly porous matrix (Dahman, 2009; Meftahi et al., 2010). However, the fibril size, surface area and porosity of BC are not absolutely constant and vary within a certain range according to the activity of the producing organism, the composition of culture media, and the variation in carbon sources used for its production (Kaewnopparat, Sansernluk, & Faroongsarng, 2008).

The water holding capacity (WHC) and water release rate (WRR) are the most important properties which are directly involved in the biomedical applications of BC as a dressing material. The proper moisture content of a dressing material accelerates the wound healing process and protects it against contamination (Kaewnopparat et al., 2008). The WHC and WRR in turn have a direct relation with the porosity and surface area of the BC matrix. In fact, the high WHC of BC is due to its very porous nature. The water resides inside the pores and is bound to the cellulose fibrils through hydrogen bonding (Gelin et al., 2007). The loose fibril arrangement, high surface area per unit mass and hydrophilic nature of BC results in a very high WHC (Dahman, 2009). BC has a wide range (100–200 times its dry weight) of WHC values (Lin, Hsu, Chen, & Chen, 2009; Schrecker & Gostomsk, 2005). This variation may be due to differences in the fibril arrangement, surface area, and porosity of different BC

* Corresponding author. Tel.: +82 53 950 5621; fax: +82 53 950 6615.
E-mail address: parkjk@knu.ac.kr (J.K. Park).

0144-8617/$ – see front matter © 2012 Elsevier Ltd. All rights reserved.
doi:10.1016/j.carbpol.2012.01.006

samples. Structural modifications affect the physico-mechanical properties of BC (Shezad, Khan, Khan, & Park, 2010; Ul-Islam, Shah, Ha, & Park, 2011). It is well known that the composition of the culture media affects the various properties of BC (Shezad et al., 2010). It has also been reported that the addition of certain additives including agar, carboxymethylcellulose, microcrystalline cellulose, and sodium alginate to the culture medium causes variation in the structural properties of BC (Cheng, Catchmark, & Demirci, 2009). Similarly, the preparation of BC composites with other materials also affects its structure and physico-mechanical properties, including variations in the pore size, surface area, WHC and WRR. For example, the average pore size of BC–Aloe vera composites was reduced five times while the surface area and WHC were increased compared to pure BC (Saibuatong & Phisalaphong, 2010).

From the literature survey, it appears that no comprehensive efforts have been made until now to determine the relationship of pore size and surface area with WHC and WRR although the porosity and WHC have been studied as the vital properties of BC (Guo & Catchmark, 2012; Hui et al., 2009; Sanchavanakit et al., 2006; Tang, Jia Shiru Jia, & Yang, 2010). As these properties are affected by variations in the structure of BC, an attempt was made in the present study to determine the relationship between porosity, surface area, WHC, and WRR by modifying the structure of BC in situ (during synthesis) and ex situ (at post-production level). This study included the investigation of these parameters for: (a) pure BC produced in a common synthetic medium, (b) BC produced by addition of various concentrations (1, 2, and 4%) of a single sugar α-linked glucuronic acid-based oligosaccharide (SSGO) to the synthetic medium, (c) composites of BC prepared with a polymer (chitosan, Ch), and (d) BC composites prepared with inorganic clay particles (montmorillonite, MMT).

2. Materials and methods

2.1. Microorganism and cell culture

Gluconacetobacter hansenii PJK (KCTC 10505BP) was grown on MAE basal medium containing glucose 10 g/L, yeast extract 10 g/L, peptone 7 g/L, acetic acid 1.5 mL/L, and succinate 0.2 g/L of distilled water (Shezad et al., 2010). The agar plates used for growing the strains were prepared by dissolving 20 g/L agar in the basal medium. The pH of the medium was adjusted to 5.0 with 1 M NaOH. The medium was sterilized for 15 min at 121 °C before use. Colonies of *G. hansenii* PJK were inoculated into 50 mL of medium in a 250 mL flask, shaken at 150 rpm and cultured at 30 °C for 24 h.

2.2. BC production

Pure BC was produced by inoculating 5.0% of *G. hansenii* PJK culture into MAE medium and kept under static conditions at 30 °C and pH 5 for 10 days in Erlenmeyer flasks (Ha, Shah, Ul-Islam, Khan, and Park, 2011). The SSGO, a by-product obtained during the BC production, was produced according to the method described by Khan, Khan, & Park (2008). BC with the addition of SSGO was prepared by adding 1, 2, and 4% SSGO to MAE medium, cultured under similar conditions and harvested by following the same procedure as for the BC. Similarly, BC sheets for the preparation of composites were produced in sterilized rectangular containers under the same culture conditions as the pure BC for 7 days. All the BC sheets were treated with 0.3 M NaOH at 121 °C for 15 min in order to disrupt and dissolve the microbial cells. The BC was then washed thoroughly with distilled water until the pH of the water became neutral. The prepared BC sheets were then stored in distilled water at 4 °C until further use.

2.3. Preparation of BC composites

The composites of BC were prepared by treating the BC sheets with Ch (Aldrich, St. Louis, USA) (BC–Ch) or MMT powder (Aldrich, St. Louis, USA) (BC–MMT). BC–Ch composites were prepared by immersing the BC sheets in 1% Ch prepared in 1% acetic acid solution under shaking conditions at 150 rpm and at 50 °C for 20 h as reported earlier (Ul-Islam et al., 2011). The solution on the surface of the BC–Ch composite sheets was removed with filter paper and finally freeze-dried at −40 °C for 2 days. BC–MMT composites were also prepared by following a similar procedure as that adopted for the BC–Ch composites. For this purpose, BC sheets were immersed in 2% aqueous suspension of MMT under shaking conditions at 150 rpm and 50 °C for 20 h followed by the removal of surface MMT suspensions and freeze-drying.

2.4. FE-SEM analysis

FE-SEM analysis was carried out in order to analyze the topography of the surface and the matrix of BC sheets. Microphotographs of the freeze-dried samples were taken using a Hitachi S-4800 & EDX-350 (Horiba) FE-SEM (Tokyo Japan). Samples were fixed on the brass holder and coated with osmic acid (OsO_4) by a VD HPC-ISW osmium coater (Tokyo Japan) prior to FE-SEM observation.

2.5. Brunauer–Emmett–Teller (BET) surface area and pore size analysis

The surface area and pore size of the various BC sheets were determined with the ASAP-2020 Surface Area and Porosity Analyzer (Micromeritics, Atlanta, GA). The samples were placed in sample cells and heated up to 348 K for 3 h in order to remove the moisture and then cooled to room temperature before the BET analysis. The BET surface area and pore size were determined through N_2 adsorption at 77 K.

2.6. Water holding capacity and water release rate

The WHC of the samples was measured by the sieve shake method. The dried BC sample sheets were immersed in distilled water for a sufficient time to completely swell up. The sheets were then taken out of the storage container using tweezers. The samples were put in a sieve and were quickly shaken twice to remove the surface water and then weighed. These samples were allowed to dry at ambient temperature and their weights were measured at different time intervals. Samples were then dried at 50 °C for 24 h in order to completely remove the water. The WHC of the different samples were calculated using the following formula (Shezad et al., 2010):

$$\text{Water holding capacity} = \frac{\text{Mass of water removed during drying } (g)}{\text{Dry weight of BC sample } (g)}$$

For determining the WRR, the wet weights of the BC samples were measured followed by continuously weighing the samples stored under ambient conditions at different time intervals until a constant dried weight was achieved. The weights of the BC samples at different time intervals were plotted against time (Shezad et al., 2010).

3. Results and discussions

In the present study, the structure of BC produced by *G. hansenii* PJK in MAE medium was modified by two different techniques, i.e., in situ (during synthesis) modification by the addition of various concentrations of SSGO to the culture media and ex situ (post-production) modification by preparing its composites. During the

Table 1
Surface area, pore diameter, pore volume and water holding capacity of in situ modified BC samples synthesized with various concentrations of SSGO and ex situ modified BC samples obtained by preparation of composites of BC with Ch and MMT.

Nature of modification	Sample	Total surface area (m^2/g)	Total pore volume (cc/g)	Average pore diameter (Å)	WHC (g water/g sample)[a]
In situ	BC0[b]	178	0.505	309	106.43 (±5.23)
	BC1[b]	168	0.144	57.12	100.36 (±4.67)
	BC2[b]	135	0.124	58.06	91.84 (±4.62)
	BC4[b]	104	0.091	49.48	85.31 (±2.23)
Ex situ	BC	285	0.728	191	121.21 (±7.81)
	BC–MMT[c]	370	0.613	74.8	84.36 (±5.04)
	BC–Ch[c]	223	0.314	116	125.84 (±6.35)

[a] Data obtained from triplicate experiments and is presented as mean ± S.D.
[b] BC0, BC1, BC2, and BC4 are the BC sheets produced with the addition of 0, 1, 2, and 4% SSGO, respectively, to the culture medium.
[c] BC–MMT and BC–Ch are the BC composites prepared with 2% montmorillonite and 1% chitosan, respectively.

in situ modifications, BC samples were produced with the addition of 1% SSGO (BC1), 2% SSGO (BC2) and 4% SSGO (BC4) to the culture medium and their morphologies, porosity, surface areas, WHC and WRR were compared to the BC produced without any addition of SSGO (BC0). Similarly, the ex situ modification included the preparation of composites of BC with Ch and MMT and their morphologies, surface properties, WHC and WRR were compared to those of the pure BC.

3.1. *Effects of in situ and ex situ modifications on the morphological characteristics of BC*

The effects of in situ and ex situ modifications on the morphology of the surface and inner matrix of BC sheets were determined through FE-SEM analysis and the results have been compiled in Figs. 1 and 2. The SEM micrographs revealed that all samples have reticulated fibril arrangements with distinct variation in the morphologies of the surface and internal matrix. Fig. 1A,C,E and G shows the surface morphology of the in situ modified BC. The thickness of the micro-fibrils increased with increasing SSGO concentration in the culture medium. More details of the structural variations can be observed from the cross sectional analysis of the in situ modified BC (Fig. 1B,D,F and H). The micrographs of cross sections show that the fibrils are loosely arranged with larger pores in the case of BC0 (Fig. 1A and B) compared to the modified BC samples. The thickness, density and compactness of micro-fibrils increased with increasing SSGO concentration in the culture medium. The BC4 has the highest compactness of fibrils (Fig. 1G and H). This increase in the fibril compactness ultimately affected the pore dimensions and resulted in a decrease in porosity of the BC sheets as shown in Fig. 1 and Table 1. The fibril thickness and density are affected by various factors including culture time, culture conditions, carbon source, inoculums amount, treatment and drying method (Guo & Catchmark, 2012; Tang et al., 2010). Cellulose chains forming sub-elementary fibrils are extruded out through small pores on the surface of the bacterial cell into the culture medium. These sub-fibrils aggregate together resulting in compact micro-fibrils (Horii, Yamamoto, & Hirai, 1997). The compactness of fibrils increases with culture time due to the secretion of more fibrils with the passage of time (Tang et al., 2010). SSGO has been shown to supplement the primary carbon source (glucose) for BC production (Ha et al., 2011). Thus the BC production continues even after the glucose is exhausted in the culture broth. This means that the BC production lasts for a relatively longer time, which causes the secretion of more micro-fibrils compared to the control. This enhanced micro-fibrils secretion increases the thickness of the BC mat and the compactness of the fibrils compared to the control. Similarly, the nature of the carbon source can also bring about structural variations in BC (Shezad et al., 2010; Tang et al., 2010) due to the production of side products that change the culture conditions, including the pH (Tang et al., 2010). SSGO is also a by-product produced during the BC synthesis by *G. hansenii* PJK (Park, Khan, & Jung, 2006; Khan et al., 2008). The addition of SSGO to the culture medium at the beginning of fermentation inhibits its self-production (Ha et al., 2011), which can ultimately affect the culture conditions and in turn brings about some variations in the physical structure of the final product. Moreover, it has also been previously reported that the addition of certain additives including agar, carboxymethylcellulose, microcrystalline cellulose, and sodium alginate to the culture medium causes variation in the structural properties of BC (Cheng et al., 2009). The current study also demonstrated that the addition of various concentrations of SSGO causes modifications in the topography of the surfaces and inner matrices of the BC sheets. Pores of various sizes and dimensions are present on the surfaces and inner matrices of different BC samples (Fig. 1). The diversity of pore sizes and shapes exists even within a single sample. However, the pore diameters cannot be determined directly from the SEM pictures.

The structure of BC was also modified ex situ (post-production) by preparing its composites with two different materials, i.e. water soluble chitosan (BC–Ch) and water suspendable MMT (BC–MMT). The FE-SEM images of pure BC as well as BC–Ch and BC–MMT composites are shown in Fig. 2, which gives details of the surface topology and the internal anatomy of these samples. These SEM micrographs revealed the effect of composite materials (Ch and MMT) on the physical structure of BC. It is worth mentioning that the BC sheets used as scaffolds for the composites and as the control were produced in the same batch. This means that the structural modifications were carried out only by the incorporation of Ch and MMT. The SEM image of pure BC (Fig. 2A) shows that the micro-fibrils are randomly arranged with plenty of spaces among them. This arrangement of fibrils results in the formation of pores with different diameters on the surface and through the entire matrix of the BC sheets. The SEM images for the cross section of the pure BC (Fig. 2B) also revealed loosely arranged micro-fibrils with abundant empty spaces throughout the entire BC matrix. Similarly, the SEM micrograph of BC–Ch (Fig. 2C) showed that the pores present on the surface of the BC sheet are almost completely filled with Ch molecules. The cross section of the BC–Ch (Fig. 2D) showed that Ch is present in the form of distinct layers or sheets in the entire BC matrix. Ch forms a strong interaction with the glucon chains of BC because both BC and Ch are organic and hydrophilic in nature (Kim et al., 2011). The BC sheets were treated with Ch present in the form of a solution; therefore, it penetrates deep into the BC matrix. The strong interactions between the Ch and BC result in modification of the physical structure of the BC, which may also lead to the changes in its physical properties (Kim et al., 2011). Moreover, the filling of empty spaces by the Ch layers ultimately results in a reduction of the total pore volume of the BC matrix as shown in Fig. 2C and D and Table 1.

The surface topology and cross section morphology of the BC–MMT composite sheets (Fig. 2E and F) are different from those

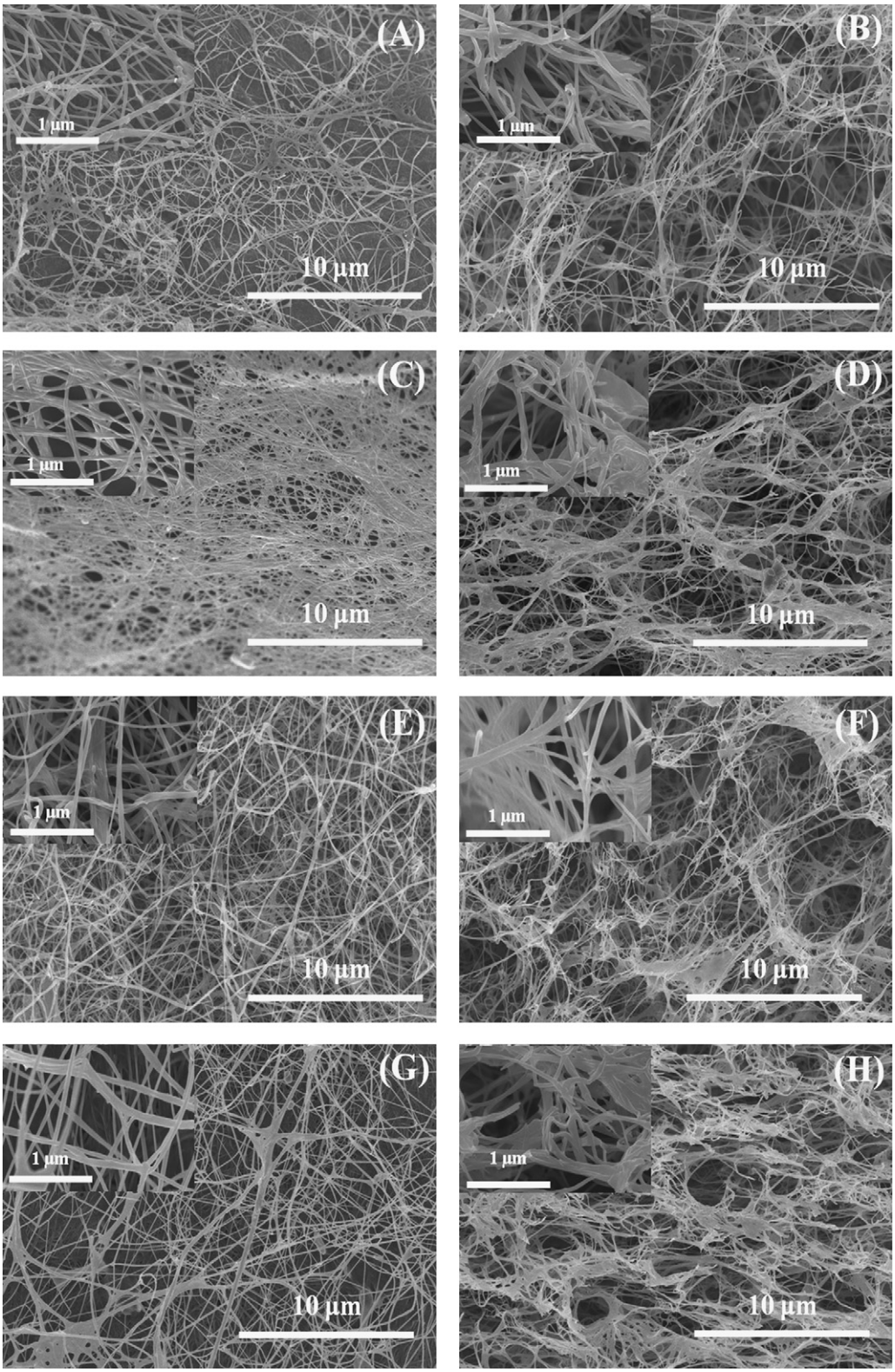

Fig. 1. FE-SEM images showing surface and cross section morphologies, respectively, for: (A, B) BC0; (C, D) BC1; (E, F) BC2; (G, H) BC4.

of BC–Ch composites. BC–MMT composites were prepared by treating the BC sheets with MMT in a suspension form, while Ch was present in a completely dissolved form during the preparation of BC–Ch composites. Therefore, the final composites have different surface and matrix topographies. The surface micrographs of BC–MMT confirm the attachment of MMT particles to the surfaces of BC sheets. The attached particles do not have a uniform size and some large particles can also be seen that may be formed by agglomeration of small MMT particles on the surfaces of BC sheets. The cross section (Fig. 2F) clearly shows the penetration of the MMT particles inside the BC matrix. In BC–MMT composites, the MMT particles penetrated into the BC matrix through the pores.

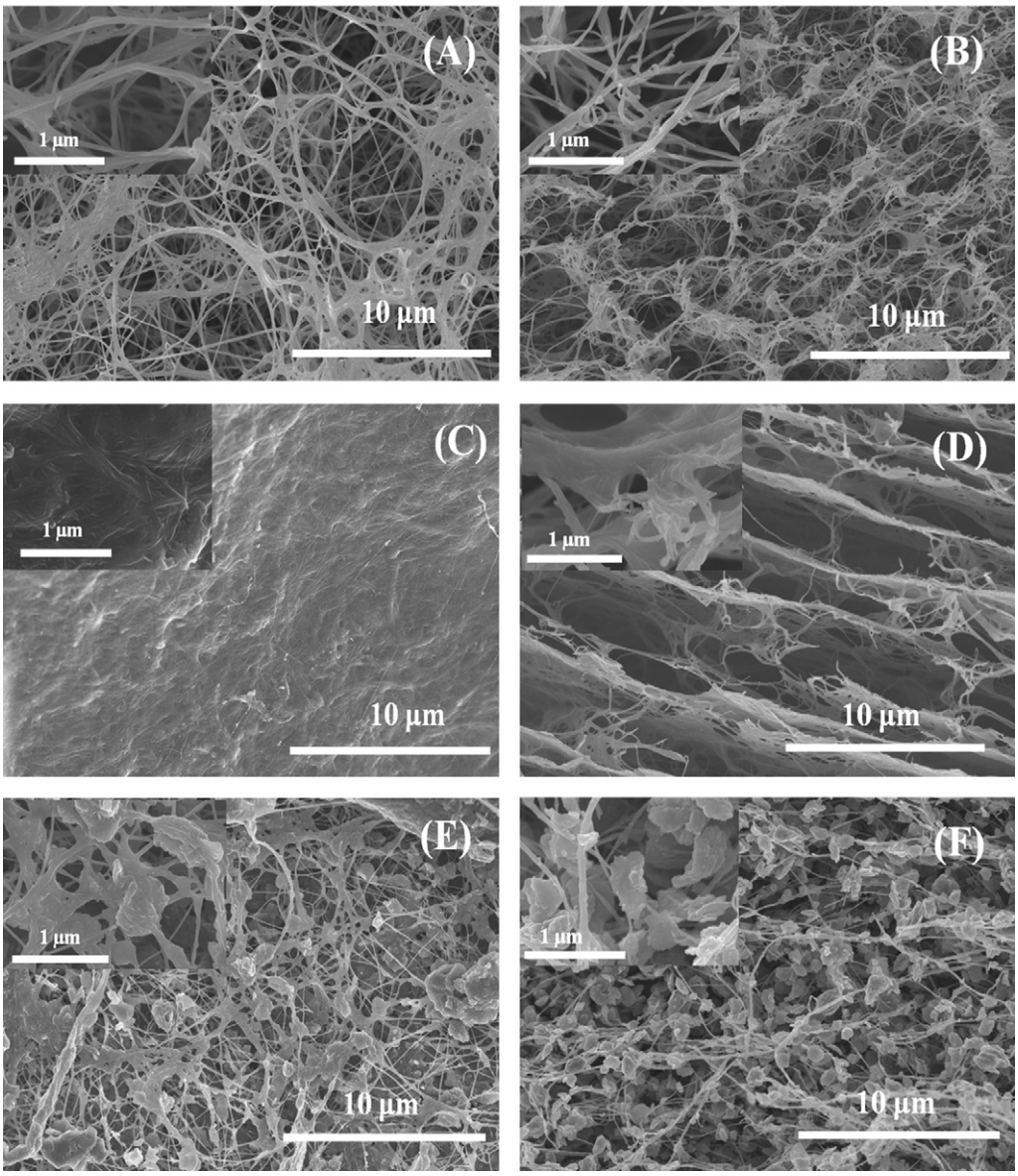

Fig. 2. FE-SEM images showing surface and cross section morphologies, respectively, for: (A, B) control BC; (C, D) BC–Ch; (E, F) BC–MMT.

The presence of hydroxyl groups in both MMT and BC can lead to organic-inorganic hydrogen bonding interactions (Darder, Colilla, & Ruiz-Hitzky, 2003; Theng, 1970). The total energy adsorbed during interactions between the individual polymer chain and clay particles is high due to the numerous points of interaction, although such interactions are weak (Theng, 1970).

3.2. Effect of in situ and ex situ modifications on pore size, pore volume and surface area of BC sheets

The overall results for the morphological characteristics of the surface and matrices of BC sheets (Figs. 1 and 2) showed that both in situ and ex situ modifications reduced the pore size and pore volume of the BC sheets. However, the pore size, pore volume and surface area could not be clearly determined from the SEM images. Therefore, these parameters were analyzed using the BET technique in order to verify the FE-SEM results and to get further information about the anatomy of the BC samples. BET is an important tool to study the surface and internal variations in physical structure by determining the surface area, total pore volume, and pore size (micro, meso and macro pores) of a sample (Guo & Catchmark, 2012).

The pore size distributions of the pure BC and BC produced in the presence of various concentrations of SSGO in the culture medium are shown in Fig. 3. It can be seen that the pore diameter and pore volume of the pure BC are much higher than those of the other BC samples. Moreover, both the pore size and pore volume decreased with increasing SSGO concentration. Table 1 shows the total surface area (m^2/g), total pore volume (cc/g), and average pore diameter (Å) of the BC samples. The total surface area for BC0 is 178 (m^2/g) which decreased to 168 (m^2/g) for BC1, 135 (m^2/g) for BC2 and 104 (m^2/g) for BC4. Similarly, the total pore volume is highest (0.505 cc/g) for BC0 among all the samples. The pore volume drastically decreased for BC1 to 0.144 (cc/g) followed by a gradual decrease for the samples prepared with higher concentrations of SSGO. The pore volumes for BC2 and BC4 were 0.124 and 0.091 (cc/g), respectively. The average pore diameter was found to be 309 (Å) for BC0, which was highest among all the BC samples. It decreased to 57.12 (Å) for BC1, 58.06 (Å) for BC2 and 49.48 (Å) for BC4. The overall results for total surface area, total pore volume and

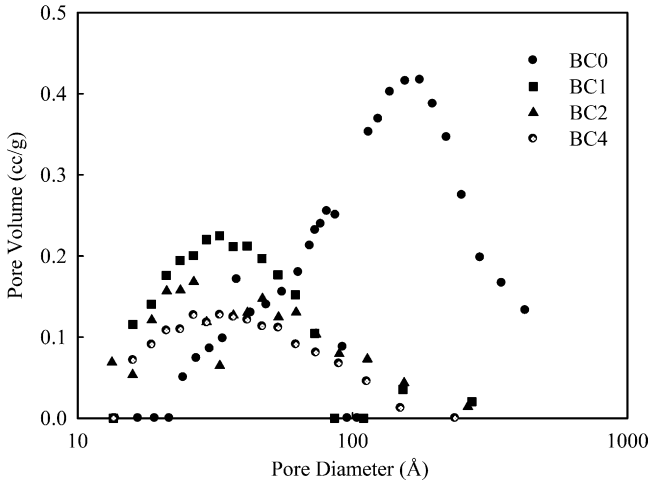

Fig. 3. Pore size distribution of control BC (BC0) and in situ modified BC (BC1, BC2 and BC4) from desorption pore volume plot by BET.

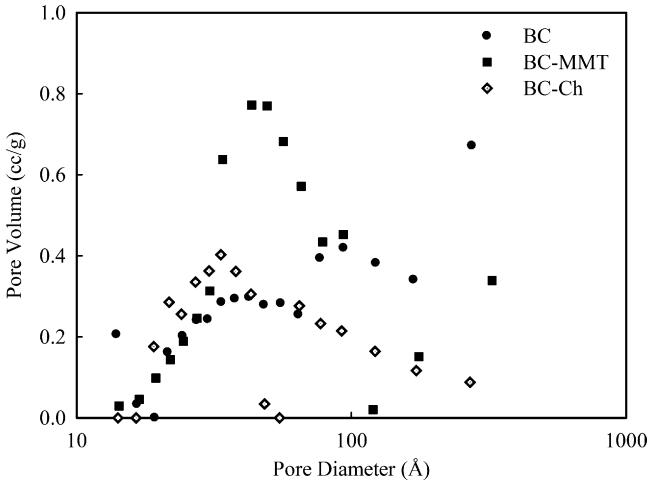

Fig. 4. Pore size distribution of control BC and the ex situ modified BC composites (BC–MMT and BC–Ch) from desorption pore volume plot by BET.

average pore diameter follow a decreasing trend with increasing SSGO concentration in the order of BC0 > BC1 > BC2 > BC4, although there was a minor deviation from this trend for the pore diameters in the cases of BC1 and BC2, as shown in Table 1. Similar trends for these parameters are also evident from the FE-SEM micrographs (Fig. 1). The results showed that the surface areas of BC sheets vary according to their porosity (Table 1). The increases in the number and size of the surface pores result in the extension of the surface area (Gao et al., 2011; Guo & Catchmark, 2012). The pore size and pore volume in the present study decreased with increasing SSGO concentration in the culture medium (Table 1). The surface area and the porosity both depend on the arrangement of fibrils. Closely arranged fibrils have lower porosity, which also decreases the total surface area (Gao et al., 2011; Guo & Catchmark, 2012). The fibrils become compact and dense with the addition of SSGO to the growth medium. This dense and compact cellulose structure results in a low surface area and porosity, as reported previously (Gao et al., 2011; Guo and Catchmark, 2012). The results also show that the BC surface and internal matrix are almost completely saturated with meso- and macropores (20–1000 Å) while only a few micropores (below 20 Å) are present in the BC matrix (Fig. 3). The total pore volume of the pure BC is higher than the rest of the samples due to the presence of pores with larger diameters (Fig. 3).

BET surface area analysis for the ex situ modified BC was carried out to determine the effects of composite preparation on the structure of BC. The results for the surface area, pore size and total pore volume of all the samples are shown in Table 1, while the pore size distribution is shown in Fig. 4. It can be seen from Table 1 that the total pore volume of the unmodified BC is 0.728 (cc/g), which is higher than the values of both the BC composites. The pore volume decreased to 0.613 (cc/g) in case of the BC–MMT composites, while it drastically decreased to 0.314 (cc/g) in the BC–Ch composites. Similarly, the average pore diameter was also lower in BC composites than in pure BC. The main reason for this decrease in the pore size and pore diameter is that the Ch and MMT penetrate inside the pores and are also attached to the surface of the BC. The nature of the penetration and surface attachments of MMT and Ch molecules to BC fibres are different from each other. The Ch, being in solution form, penetrates easily into the empty pores of the BC, resulting in uniform filling of the pores from all sides in a similar way to that reported previously (Kim et al., 2011; Ul-Islam et al., 2011). This type of compact filling in the pores leads to a significant reduction in pore size and volume. The pore filling and subsequent decrease in the pore size in BC–Ch composites can also be clearly seen in the SEM micrographs in Fig. 2C and D. On the other hand, the MMT, being insoluble in water, is present as suspended particles. These solid particles cannot easily penetrate into the pores of the BC matrix, which results in a less homogenous packing than for the Ch molecules. In a nutshell, the internal pores in the case of BC–MMT composites are not completely filled and thus they have a relatively larger total pore volume as compared to BC–Ch composites. The composite formation, however, leads to a decrease in pore size in both the BC–Ch and BC–MMT as compared to the pure BC (Table 1), which is also evident from the SEM microphotographs in Fig. 2. Table 1 also shows the variation in total surface area with the formation of BC composites. The total surface area for the control BC was 285 m^2/g. The surface area was higher (370 m^2/g) for BC–MMT and lower (223 m^2/g) for BC–Ch composites than it was for the control BC. The lower surface area in the case of BC–Ch composites is probably due to the strong interactions between the BC chains and Ch molecules (Kim et al., 2011; Ul-Islam et al., 2011), which ultimately lead to a more compact filling of the pores in the BC matrix and thus a reduction of the empty spaces. Moreover, these stronger interactions may bring the fibres closer and reduce the volume per unit mass of the samples, which ultimately results in a decrease in surface area of the BC–Ch composites. On the other hand, the surface area of the BC–MMT composites was higher than that of the pure BC (Table 1), which may be due to the irregular arrrangement of MMT particles on the surfaces of BC sheets. The adsorption of these particles forms a rough coating on the surfaces of the BC sheet which results in an increase of the surface area similar to that reported for Aloe vera-BC composites (Saibuatong & Phisalaphong, 2010). MMT particles cover the surface of the BC sheet from all sides and increase the exposed surface. The pore size distributions for all three samples have been shown in Fig. 4 and are in agreement with the results given in Table 1.

3.3. *Water holding capacity and water release rate analysis of pure and modified BC*

The modifications in the physical structure of BC are likely to bring changes to its physical characteristics. The WHC and WRR are the most important properties which are directly involved in the biomedical applications of BC as a dressing material. The proper moisture content of a dressing material accelerates the wound healing process and protects it against contamination (Cienchanska, 2004; Ul-Islam et al., 2011), as well as facilitating the penetration of active substances into the wound and enabling an easy and painless dressing change without damage to the newly formed skin (Shezad et al., 2010). Therefore, the determination of the effects of in situ

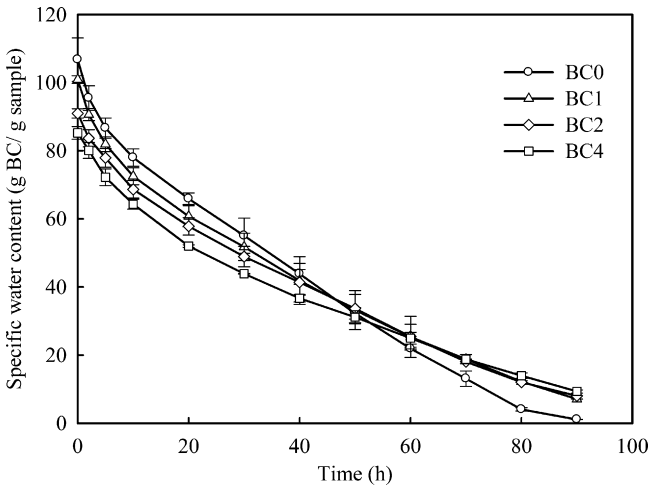

Fig. 5. Water retention rate of bacterial cellulose samples of control BC (BC0) and in situ modified BC (BC1, BC2 and BC4).

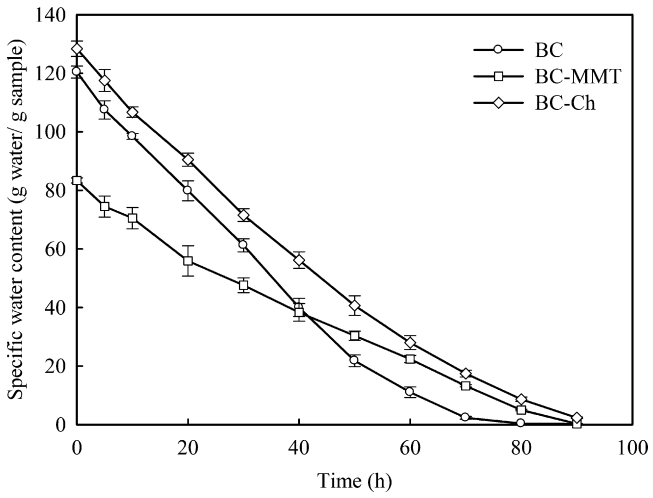

Fig. 6. Water retention rate of bacterial cellulose samples of control BC and in situ modified BC composites (BC–MMT and BC–Ch).

and ex situ modifications of BC structure on the WHC and WRR was a major aim of the present study.

Table 1 shows the WHC of pure BC and in situ modified BC prepared with the addition of various concentrations of SSGO. The WHC of BC0 is 106.43 times its dry weight, which is higher than all the in situ modified BC samples. The WHC for BC1 was 100.36, while it was 91.84 for BC2 and for BC4 it was 85.31 times its dry weight. From Table 1, it can be deduced that WHC decreases with increasing SSGO concentration in the culture medium. The WHC for the BC samples were in the order BC0 > BC1 > BC2 > BC4. The variation in the WHC of these BC samples can be attributed to their respective porosity and surface areas. The water molecules are trapped physically on the surface and inside the BC matrix consisting of reticulated fibrils (Watanabe, Tabuchi, Morinaga, & Yoshinaga, 1998). If there are plenty of empty spaces among the BC fibrils then more water can penetrate and adsorb onto the material. Thus, the greater the surface area and the larger the pore size, the greater will be the WHC of the BC sample (Guo & Catchmark, 2012; Meftahi et al., 2010). The results obtained in the present study showed that the surface area, pore size and pore volume decrease with increasing SSGO concentration in the medium (Table 1). The decrease in the WHC also follows the same trend. The trend of the WRR for pure and in situ modified BC samples is different from that of their WHC. The WRR was determined for all the BC samples until 90 h and the results have been displayed in Fig. 5. It was revealed that initially the evaporation rates of water molecules from all the samples were similar because the water on the surface of the BC sheets escapes at similar rates from these samples. However, with the passage of time the WRR slows down for the in situ modified BC prepared with different concentrations of SSGO, compared to the pure BC for which the WRR remained nearly constant until the end of the experiment (Fig. 5). The absorbed water almost completely evaporated in 90 h from the control BC while the modified BC samples contained a reasonable amount of water at this time period. The final water content was dependent on the concentration of SSGO added to the culture medium although the differences were not very significant. The higher the concentration of SSGO the larger was the final water content after 90 h, as shown in Fig. 5. However, the reverse of this trend was true for the WHC of these samples (Table 1). These results can be explained on the basis of FE-SEM (Fig. 1) and pore size (Table 1) analysis of these samples. The escape of the water molecules from the BC matrix to the environment mainly depends on the arrangement of its micro-fibrils (Shezad et al., 2010). Closely arranged micro-fibrils bind the water molecules more efficiently due to the stronger hydrogen bonding interactions, as compared to the loosely arranged micro-fibrils, which are relatively ineffective at protecting the water from evaporation (Ougiya, Watanabe, Matsumura, & Yoshinaga, 1998; Shah, Ha, & Park, 2010). The micro-fibrils in BC0 are expanded with plenty of gaps between them as shown in Fig. 1, which leads to a higher pore size (Table 1) and thus a higher WRR (Fig. 5). On the other hand, the micro-fibrils in BC4 are more crowded (Fig. 1G and H) which leads to a smaller pore volume and pore size (Table 1). This means that BC4 can protect the water molecules more efficiently from evaporation, which results in a slow WRR (Fig. 5) and thus BC4 has the highest water content after 90 h. The overall order of water retention for the tested samples is BC4 > BC2 > BC1 > BC0. In conclusion, both the WHC and WRR for the in situ modified BC are highly dependent on the structural features of the BC, especially the pore size and total pore volume. BC samples with smaller pore sizes can retain water in the matrix for longer times, but a high pore volume means that a sample can accumulate more water, increasing the WHC of the sample.

The results for the WHC and WRR of the ex situ modified BC samples through the preparation of composites are shown in Table 1 and Fig. 6, respectively. The results showed that the pure BC absorbed 121.21 times its dry weight of water. The WHC slightly increased to 125.84 in BC–Ch composites compared to pure BC, as shown in Table 1. The pore size of BC–Ch was smaller compared to that of the pure BC. However, Ch being a highly hydrophilic compound interacts with the water molecules and BC chains simultaneously. These interactions increase the adsorption of water molecules into the composite matrix (Kim et al., 2011; Ul-Islam et al., 2011) and thus the WHC of the BC–Ch composite is slightly higher than that of the pure BC. In contast to BC–Ch composites, the WHC of the BC–MMT composite is 84.36 which is quite a lot lower than that of the pure BC. This may be due to the presence of MMT particles on the surface and inside the BC matrix, which reduces the space for penetration and adsorption of water molecules. MMT particles have the ability to absorb water and thus swell up several times (Ikari, Saffer, & Marone, 2007) but the ratio of water absorption by the MMT particles to the increase in the dry weight of BC–MMT composites is much lower and thus the WHC of the composite is also lower compared to the pure BC. Furthermore, the total pore volume of the BC–MMT is smaller than that of pure BC (Table 1), which leads to the adsorption of a smaller quantity of water. The results for the WRR of the pure BC and ex situ modified BC samples are given in Fig. 6. The WRR for these samples were determined over a time of 90 h. It can be seen from Fig. 6 that

the water molecules escaped very rapidly from the surface of the pure BC and the evaporation was almost finished (more than 97%) in 70 h. In contrast to the pure BC, it took about 90 h for the complete evaporation of water from the surfaces of both BC–Ch and BC–MMT composites. The pore size is smaller in these composites (Table 1 and Fig. 2) and thus the penetrated water molecules are more tightly sandwiched between the micro-fibrils. Furthermore, the surface covering of the BC by Ch or MMT provides a hurdle for the escape of water molecules from these composites (Ul-Islam et al., 2011). All these factors collectively result in the retardation of water evaporation from the BC matrix and thus decrease the WRR. This means that the water molecules will reside for a longer time in the BC matrices of composites (Fig. 6). It can be concluded that both the WHC and WRR for the ex situ modified BC are highly dependent on the nature and arrangement of the composite material on the surface and inside the matrix rather than the structural features of the BC.

4. Conclusion

In the present study, the variations in the physical properties of BC such as WHC and WRR were correlated to the changes in different parameters, including micro-fibril arrangements, pore size, pore volume and surface area after structural modification. The fibril arrangement became denser while the pore size and pore volume decreased with increasing SSGO concentration. The pore size and volume also decreased in BC composites due to the filling of pores by MMT and Ch. The WHC and WRR increased with increases in pore volume and pore size in in situ modified BC, while in ex situ modified BC the WHC and WRR were dependent on the nature and arrangement of the composite material on the surface and inside the matrix of the BC sheets.

Acknowledgment

This research was supported by Basic Science Research Program through the National Research Foundation of Korea (NRF) funded by the Ministry of Education, Science and Technology (NRF-2010-0012672).

References

Cheng, K.-C., Catchmark, J. M., & Demirci, A. (2009). Effect of different additives on bacterial cellulose production by *Acetobacter xylinum* and analysis of material property. *Cellulose*, *16*, 1033–1045.

Choi, C. N., Song, H. J., Kim, M. J., Chang, M. H., & Ki, S. J. (2009). Properties of bacterial cellulose produced in a pilot-scale spherical type bubble column bioreactor. *Korean Journal of Chemical Engineering*, *26*, 136–140.

Cienchanska, D. (2004). Multifunctional bacterial cellulose/chitosan composite materials for medical applications. *Fibres and Textiles in Eastern Europe*, *12*, 69–72.

Czaja, W., Krystynowicz, A., Bielecki, S., & Brown, R. M. (2006). Microbial cellulose-the natural power to heal wounds. *Biomaterials*, *27*, 145–151.

Czaja, W., Young, D. J., Kawechi, M., & Brown, R. M. (2007). The future prospects of microbial cellulose in biomedical applications. *Biomacromolecules*, *8*, 1–12.

Dahman, Y. (2009). Nanostructured biomaterials and biocomposites from bacterial cellulose nanofibers. *Journal of Nanoscience and Nanotechnology*, *9*, 5105–5122.

Darder, M., Colilla, M., & Ruiz-Hitzky, E. (2003). Biopolymer-clay nanocomposites based on chitosan, intercalated in montmorillonite. *Chemistry of Materials*, *15*, 3774–3780.

Gao, C., Wan, Y., Yang, C., Dai, K., Tang, T., Luo, H., & Wang, J. (2011). Preparation and characterization of bacterial cellulose sponge with hierarchical pore structure as tissue engineering scaffold. *Journal of Porous Materials*, *18*, 139–145.

Gelin, K., Bodin, A., Gatenholm, P., Mihranyan, A., Edwards, K., & Stromme, M. (2007). Characterization of water in bacterial cellulose using dielectric spectroscopy and electron microscopy. *Polymer*, *48*, 7623–7631.

Guo, J., & Catchmark, J. M. (2012). Surface area and porosity of acid hydrolyzed cellulose nanowhiskers and cellulose produced by *Gluconacetobacter xylinus*. *Carbohydrate Polymers*, *87*, 1026–1037.

Ha, J. H., Shah, N., Ul-Islam, M., Khan, T., & Park, J. K. (2011). Bacterial cellulose production from a single sugar α-linked glucuronic acid-based oligosaccharide. *Process Biochemistry*, *46*, 1717–1721.

Horii, F., Yamamoto, H., & Hirai, A. (1997). Microstructural analysis of microfibrils of bacterial cellulose. *Macromolecular Symposia*, *120*, 197–205.

Hui, J., Yuanyuan, J., Jiao, W., Yuan, H., Yuan, Z., & Shiru, J. (2009). Potentiality of bacterial cellulose as the scaffold of tissue engineering of cornea. In R. Shi (Ed.), *Proceedings of the 2nd international conference on biomedical engineering and informatics* Tianjin, China, (pp. 1–5). Institute of Electrical and Electronics Engineers.

Ikari, M. J., Saffer, D. M., & Marone, C. (2007). Effect of hydration state on the frictional properties of montmorillonite-based fault gouge. *Journal of Geophysical Research*, *112*, B06423. doi:10.1029/2006JB004748

Kaewnopparat, S., Sansernluk, K., & Faroongsarng, D. (2008). Behavior of freezable bound water in the bacterial cellulose produced by *Acetobacter xylinum*: An approach using thermoporosimetry. *American Association of Pharmaceutical Scientists*, *9*, 701–707.

Khan, T., Khan, S., & Park, J. K. (2008). Simple fed-batch cultivation strategy for the enhance production of a single-sugar glucoronic acid-based oligosaccharides by a cellulose producing *Gluconacetobacter hansenii* strain. *Biotechnology Bioprocess Engineering*, *13*, 240–247.

Kim, J., Cai, Z., Lee, H. S., Choi, G. S., Lee, D. H., & Jo, C. (2011). Preparation and characterization of a bacterial cellulose/chitosan composite for potential biomedical application. *Journal of Polymer Research*, *18*, 739–744.

Klemn, D., Schumann, D., Udhardt, U., & Marsch, S. (2001). Bacterial synthesized cellulose artificial blood vessels for microsurgery. *Progress in Polymer Science*, *26*, 1561–1603.

Li, H. X., Kim, S. J., Lee, Y. W., Kee, C. D., & Oh, K. (2011). Determination of the stoichiometry and critical oxygen tension in the production culture of bacterial cellulose using saccharified food wastes. *Korean Journal of Chemical Engineering*, *28*, 2306–2311.

Lin, S. B., Hsu, C. P., Chen, L. C., & Chen, H. H. (2009). Adding enzymatically modified gelatin to enhance the rehydration abilities and mechanical properties of bacterial cellulose. *Food Hydrocolloids*, *23*, 2195–2203.

Meftahi, A., Khajavi, R., Rashidi, A., Sattari, M., Yazdanshenas, M. E., & Torabi, M. (2010). The effect of cotton gauze coating with microbial cellulose. *Cellulose*, *17*, 199–204.

Nasab, M. M., & Yousef, A. R. (2010). Investigation of physicochemical properties of the bacterial cellulose produced by *Gluconacetobacter xylinus* from date syrup. *World Academy of Science, Engineering and Technology*, *68*, 1248–1253.

Ougiya, H., Watanabe, K., Matsumura, T., & Yoshinaga, F. (1998). Relationship between suspension properties and fibril structure of disintegrated bacterial cellulose. *Bioscience, Biotechnology, and Biochemistry*, *62*, 1714–1719.

Park, J. K., Khan, T., & Jung, J. Y. (2006). Structural studies of the glucuronic acid oligomers produced by *Gluconacetobacter hansenii* strain. *Carbohydrate Polymers*, *63*, 482–486.

Phisalaphong, M., Suwanmajo, T., & Sangtherapitiku, P. (2008). Novel nanoporous membranes from regenerated bacterial cellulose. *Journal of Applied Polymer Science*, *107*, 292–299.

Saibuatong, O. A., & Phisalaphong, M. (2010). Novo aloe vera-bacterial cellulose composite film from biosynthesis. *Carbohydrate Polymers*, *2*, 455–460.

Sanchavanakit, N., Sangrungraungroj, W., Kaomongkolgit, R., Banaprasert, T., Pavasant, P., & Phisalaphong, M. (2006). Growth of human keratinocytes and fibroblasts on bacterial cellulose film. *Biotechnology Progress*, *22*, 1194–1199.

Schrecker, S. T., & Gostomsk, P. A. (2005). Determining the water holding capacity of microbial cellulose. *Biotechnology Letters*, *27*, 1435–1438.

Shah, N., Ha, J. H., & Park, J. K. (2010). Effect of reactor surface on production of bacterial cellulose and water soluble oligosaccharides by *Gluconacetobacter hansenii PJK*. *Biotechnology and Bioprocess Engineering*, *15*, 110–118.

Shezad, O., Khan, S., Khan, T., & Park, J. K. (2009). Production of bacterial cellulose in static conditions by a simple fed-batch cultivation strategy. *Korean Journal of Chemical Engineering*, *26*, 1689–1692.

Shezad, O., Khan, S., Khan, T., & Park, J. K. (2010). Physicochemical and mechanical characterization of bacterial cellulose produced with an excellent productivity in static conditions using a simple fed-batch cultivation strategy. *Carbohydrate Polymers*, *82*, 173–180.

Tang, W., Jia Shiru Jia, Y., & Yang, H. (2010). The influence of fermentation conditions and post-treatment methods on porosity of bacterial cellulose membrane. *World Journal Microbiology Biotechnology*, *26*, 125–131.

Theng, B. K. G. (1970). Interactions of clay minerals with organic polymers. Some practical applications. *Clays and Clay Minerals*, *18*, 357–362.

Ul-Islam, M., Shah, N., Ha, J. H., & Park, J. K. (2011). Effect of chitosan penetration on physico-chemical and mechanical properties of bacterial cellulose. *Korean Journal of Chemical Engineering*, *28*, 1025–1031.

Wan, W. K., Hutter, J. L., Millon, L., & Guhados, G. (2006). Bacterial cellulose and its nanocomposites for biomedical applications. *ACS Symposium Series*, *938*, 221–241.

Watanabe, K., Tabuchi, M., Morinaga, Y., & Yoshinaga, F. (1998). Structural features and properties of bacterial cellulose produced in agitated culture. *Cellulose*, *5*, 187–200.